RSC Advances

Cellulose nanofibres from rice straw: process development for improved delignification and better crystallinity index by statistical optimization

Journal:	*RSC Advances*
Manuscript ID	Draft
Article Type:	Paper
Date Submitted by the Author:	n/a
Complete List of Authors:	Sharma, Amita; Center of innovative and applied bioprocessing, Chemical engineering goswami, Saswata; Center of innovative and applied bioprocessing , Chemical Engineering Mandal, Tamal ; National Institute of Technology, Chemical engineering
Subject area & keyword:	Biomaterials < Materials

RSC Advances

ARTICLE

Cellulose nanofibres from rice straw: Process development for improved delignification and better crystallinity index by statistical optimization

Received 00th January 20xx,
Accepted 00th January 20xx

DOI:
10.1039/x0xx00000xwww.rsc.org/

Amita Sharma[1], Tamal Mandal[2] and Saswata Goswami[1]*

The effects of alkaline pretreatment and delignification methodology on rice straw to yield cellulose nanofibres (CNF) have been investigated. Rice straw was treated with 12 wt % NaOH. As a result alkaline cellulose fibres (ACF) were derived at 31 % yield. Further delignification of ACF with 5 wt % of sodium chlorite resulted in α cellulose. For all these operations of pretreatment and delignification, protocols have been optimized by Response Surface Methodology. Subsequent mechanical treatment with high pressure homogenization converted α cellulose into nanocellulose with minimum lignin content of 1.32%. The confirmation of removal of hemicellulose and lignin was supported by the FTIR and TGA studies. The dimensions of the nanocellulose particles derived from rice straw was found to be in the nano dimensions range of 10 nm to 50 nm as observed by Transmission Electron Microscopy (TEM).

Introduction

Agricultural residues, postharvest agro residues such as rice straw, wheat straw, banana rachis, sisal, kapok are abundant lignocellulosic bio based feedstock to valorize, both for the purpose of nonedible material preparation as well as for the green impact towards the environment.[1] In India rice is a widely grown crop that leaves substantial quantity of postharvest straw in the field. Rice straw (dry stalks of rice) can be defined as an underutilized by-product. Current uses of rice straw include fuel for cooking, animal bedding, animal feed, building materials and composting. But majority of rice straw about 70-80 MMT is disposed off by burning. However rice straw burning causes lung and respiratory diseases to the human being, soil erosion and climatic changes due to Greenhouse gas emission effect. That's why rice straw valorization is the imminent priority to the scientists. In India and South Asian countries rice straw is available, at 1.0 to 1.5 kg per kg of rice grain harvested, and they are the most abundant lignocellulosic biomass to be converted to cellulosic nanomaterials such as CNC (cellulose nanocrystals) and CNF (and its bio- nanocomposites derivatives for several versatile practical applications).[2]

In recent decades nanocellulose has become an attractive choice for several end users due to their exceptional mechanical, thermal, and biological properties.[3] Nanocellulose is non–toxic, completely biodegradable and biocompatible and it doesn't create any adverse effect on health and environment. Nanocelullose is much favorable because of its low thermal expansion coefficient, high aspect ratio, better tensile strength, good mechanical and optical properties. There are many more applications of its bio-nanocomposites in thermo-reversible and tenable hydrogels,[4] paper making, coating additives, food packaging, flexible screens, optically transparent films and light-weight materials for ballistic protection, food packaging and automobile windows,[5,6] and gas barriers. It finds great potential in biopharmaceutical applications such as in drug delivery.[7] Its nanocomposites (stronger biomaterials formed by the copolymerization with PHB) are the materials for fabricating temporary implants (sutures, artificial pericardia, stents etc.).
For the bio refinery of cellulose, to fractionate all the components from rice straw, intensive studies have been done on the chemistry of rice straw.[8] Usually rice straw comprises of cellulose (32-47%), hemi cellulose (19-27%),lignin (11-24%), as well as significant amount of silica (7-20%). Hemicelluloses are mainly heteropolymer of pentoses (xylose and arabinose) and hexoses (glucose, galactose, mannose) and sugar acids (acetic) whereas Lignin is a racemic, heteropolymer consisting of three hydroxycinnamyl alcohol monomers p-coumaryl, coniferyl and sinapyl alcohols. It is basically amorphous in nature, and holds together cellulose and hemicellulose fibers and gives support, resistance to the plants.[9]
Traditionally, cellulose nanofiber has been defined as purely crystalline cellulose chains having diameters within the range of 5 to 40 nm with lengths of a few microns. The process of extraction of cellulose from these regions, and consequently the process of size reduction to diameter of nano scales causes the better reinforcement properties of nanocellulose because of its greater tensile strength and aspect ratio.

Based on the applications and types of pretreatment, the extraction techniques have generally been divided into three distinct categories, including physical, chemical, and biological pretreatment. Chemical pretreatment is the most studied technique among these categories.[10,11] Chemical pretreatments that have been studied to date have had the primary goal of improving the biodegradability of cellulose by removing lignin and or hemicelluloses. Combination of two or more techniques from the same or different categories is also common.[12]

Among other methods, mechanical treatments, such as cryocrushing[13], grinding, high pressure steam treatments[14] and

homogenization,[15] chemical treatments, such as acid hydrolysis[16, 17], ionic liquid,[18] biological treatments, such as enzyme-assisted hydrolysis[19] and TEMPO-mediated oxidation,[20,21] chemomechanical methods and synthetic and electro spinning methods[22] as well as a combination of two or several of the aforementioned methods. Studies have also been done to optimize pretreatment conditions in rice straw [23,24,25,26] but quality and yield of nanocellulose as well as energy required are among the issues remain to be resolved.

In this work, CNF was derived from rice straw using alkali pretreatment, sodium chlorite delignification coupled with homogenization. The major emphasis of the present work lies in the application of Response Surface Methodology (RSM), a statistical approach for the parameter optimization. For alkali pretreatment step, three factors chosen as temperature (^{0}C), time (minutes) and alkali concentration (in wt%) and for each factors three levels had been taken into consideration. The optimal conditions were found to be (120 ^{0}C, 90 minutes and 12 wt % alkali solution). In case of delignification the optimal conditions were found to be (70 ^{0}C, 60 minutes, 5 wt %) by RSM. Mechanical treatment was given to the optimally treated α cellulose by the probe sonicator followed by homogenization to obtain nanocellulose. The chemical composition of cellulose , hemicelluloses and lignin in the rice straw at different stages were analysed by TAPPI T 203 cm-99 for α cellulose and Laboratory Analytical Procedures (LAP 009) for lignin. The increase of α cellulose content from 40 % to 90 % and drop in hemicellulose (31% to 5 %) and lignin content from 21.5% to 1.32% respectively confirmed the optimized process satisfactory. The confirmation of removal of hemicellulose and lignin was also supported by FTIR and TGA studies. The characterization of nanocellulose by SEM, AFM and TEM revealed that the nanocellulose diameter got shorter (10-150 nm) with the treatment. The main outcome of this work is that the CNF has been derived with minimum lignin content of 1.32% by optimized process and of better crystallinity index of 92%.

Experimental details

Materials

Rice straw was collected from local farm in Mohali, Punjab, India. It was washed and dried to remove any impurities or dust. It was ground using commercial grinder (Kinematica PX-MFC 90 D). All chemicals i.e. sodium chlorite ($NaClO_2$, 80%, technical grade, Sigma Aldrich), sodium hydroxide pellets purified (CDH), acetic acid glacial (100 %, GR, Merck) were used as received.

Alkaline treatment

The grinded rice straw was soaked in different concentrations of NaOH (8–16%) and then heated to 90-160°C for 60-120 minutes to remove hemicelluloses and some portion of lignin. The fibre to liquid ratio of the NaOH solution and rice straw was 1:20. The residue obtained was then subsequently washed with distilled water to remove the impurities. Residual mass ACF was further dried overnight at 50 ^{0}C in oven.

Isolation of α cellulose by delignification

The pretreated residue obtained was treated with optimized (2.5-5 wt %) acidified sodium chlorite at 70-85 ^{0}C for 60-120 minutes. pH was maintained in the range of 3-5 (adjusted with 1 M glacial acetic acid). At the end of the reaction, α cellulose obtained was washed with distilled water until the pH became neutral. α Cellulose obtained was dried in oven overnight at 50 ^{0}C.

Preparation of nanocellulose

α Cellulose as obtained earlier was sonicated in (Q sonica Sonicator with probe) for 10 minutes in ice bath to avoid the overheating. The suspension was further homogenized (IKA @T25 digital ULTRA TURRAX) to obtain the product as cellulose nanofibres (CNF). The product was stored in refrigerator at (-80 ^{0}C) followed by freeze drying in laboratory freeze dryer (Delta 2-24 LSCplus).

Chemical compositions of fibers

α-cellulose content was estimated according to the TAPPI T 203 cm-99. Carbohydrates, fractional compositional analyses of acid soluble lignin and acid insoluble lignin were characterized by Laboratory Analytical Procedures (LAP) of National Renewable Energy Laboratory (LAP 009). The Carbohydrate content in the fiber was determined on a high performance liquid chromatography (HPLC) System (Agilent Technologies 1200 infinity series) equipped with a Hi-Plex, H analytical column (300 mm length; 8 lm porosity) under the following conditions : flow rate , 0.7 ml/min , mobile phae , 5 mM H_2SO_4; detector RI , detector temperature, 55 ^{o}C; column temperature, 60 ^{o}C and residence time, 60 min. Prior to HPLC injection, all samples were neutralized with sodium hydroxide to achieve neutral pH and filtered through 0.2 µm nylon filters (Millipore Corporation).

Characterizations.

Fourier transform infrared spectroscopy (FTIR). The FTIR spectra of samples before and after treatment were recorded on an instrument (Agillent Technologies Cary 600) in the range of 400-4500 cm^{-1} with a resolution of 4 cm$^{-1.}$.

Thermogravimetric analysis (TGA). The thermogravimetric analysis of the fibres were conducted in a temperature interval of 25-800 ^{0}C under nitrogen atmosphere at heating rate of 10 ^{0}C per minute. Mettle Toledo thermal analyser was used for the study.

Scanning electron microscopy (SEM). Surface morphological differences were examined using a benchtop scanning electron microscope (JEOL JCM 6000 Nikon Corporation) at an acceleration voltage of 10.0 kV. Before scanning, the solid fibers were coated with gold in a smart coater (25 mm stub size).

X-ray diffraction (XRD). Crystallintiy of the solid fibers was acquired using X-ray diffractogram (XPERT-PRO D8 Bruker) equipped with CuKα (λ=0.154) in the 2 Θ range 5-40 ^{0}, (generator power settings: 40 kV and 40 mA. The empirical method was used to obtain the crystallinty index, [27] X_c of samples as shown in Eq. (1)I_{002}

$$X_{c=} \frac{I_{002} - I_{am}}{I_{002}} X100 \quad (1)$$

Where I_{002} and I_{am} are the peak intensities of crystalline and amorphous materials, respectively.

Scherrer Eq. (2) is used to calculate the crystalline size

$$\tau = \frac{\kappa\lambda}{\beta \cos\theta} \quad (2)$$

τ is the crystal dimension perpendicular to the diffracting planes with Miller Indices of hkl, λ is the wavelength of the X-ray radiation (λ = 0.154 Å) and $\beta_{1/2}$ is the full width at half maximum (FWHM) of the diffraction peaks.[28]

High resolution Transition electron moicroscopy: HR-TEM images of the cellulose nanofibers and nanofiber bundles were collected using a FEI Tecnai F20 at a accelerating voltage of 120 kV. Drops of dilute cellulose nanofiber suspensions (1 ml, 0.01 wt%) were mildly ultrassonicated in a water bath sonicator for 5 mins, deposited onto glow-discharged, carbon-coated, electron microscopy grids. The excess liquid was removed by a piece of filter paper followed by drying at room temperature.

Optimization of parameters for pretreatment and delignification. RSM is a statistical tool for designing experiments, building empirical models, and evaluating the effects of factors. RSM can reduce the number of experimental trials needed to evaluate multiple parameters and their interactions. The design and analysis of the experiments used the Design Expert software (Stat-Ease Inc, USA; trial version 9).

Pretreatment. In view of the results of the earlier work reported on rice straw, the following three factors were examined through a central composite design: the concentration of sodium hydroxide, temperature and time of reaction as shown in supporting information Table S1.[29-35] Each factor varied at three levels: concentration of sodium hydroxide (wt %) 2.5-5, Time (mins) 60-120 minutes, Temperature 90-160 (^{o}C). The response was the residual lignin content in %. A full factorial central composite design with 2^3 (8) runs , 6 center points and 6 star points was used. This led to a total of 20 experiments (Table S2). The response (lignin content) was determined experimentally for each run and compared with the predicted one obtained through central composite design.

Delignification. Similarly for delignification, the following three factors were examined through a central composite design: the concentration of sodium chlorite, temperature and time of reaction as shown in Table S3. [36-42] Each factor varied at three levels : Concentration of sodium chlorite (wt %) 2.5-5 , Time (mins) 60-120 minutes, Temperature 70-85 (^{o}C). The response was the residual lignin content in %. A full factorial central composite design with 2^3 8 runs , 6 center points and 6 star points was used. This led to a total of 20 experiments (Table S4). The response (lignin content) was determined experimentally for each run and compared with the predicted one obtained through central composite design.

Validation of the response surface model. The predicted optimal values of the factors were identified using the response surface model and the point prediction of design expert software. Validation experiments were run in triplicate at the optimal conditions. The measured response was compared to the predicted response to validate the optimal values.

Results and discussion

Pretreatment

Response surface methodology using central composite design was employed to determine the optimal levels of the three selected factors that affected the residual lignin content.

The relevant factors were the concentration of sodium hydroxide, temperature and time of reaction. Each factor was tested at three levels. The center point levels were kept at the values found to be optimal via the one-at-a-time variation of factors.

The response surface model was as follows:

Lignin (%) = 11.41 + 5.73A +3.21 B – 2.87C-3.33AB + 1.83AC + 0.39 BC + 6.04A^2 – 3.84B^2 +6.53C^2... (3)

Where A is the Temperature in ^{0}C, B is the time in minutes, C is the Concentration of sodium hydroxide in wt % (Table S5).

The least residual lignin content of 8.19 % was measured in run 16 (Table S2) with the predicted value 10.79 %. The ANOVA of the response surface model (Eq. (3)) is shown in Table S6. The F-value for the model (i.e. Eq. (3)) was 27.50 (Table S6), suggesting that the model was significant and the probability of the F-value of the model being due to experimental noise was less than 0.01% (Table S6). The temperature of the reaction, concentration of sodium hydroxide and time taken for the reaction had a significant effect on the response, P-value < 0.05 (Table S6). Moreover, the interactive effect of all the factors was also significant except for the interaction between time and concentration. The R^2 value indicates the degree to which the model was able to predict the response. The closer the R^2 value is unity, the better the model can predict the response. The determination coefficient (R^2) of the model (Eq. (3)) was 0.9612, therefore the model could explain >96% of the variation in the predicted response of the lignin content. In the case when P value is smaller than 0.05, the parameters are considerably varied and the analysis result is statistically significant value.[43] In this case, the data from ANOVA (Table S6) also showed that P value was very low, smaller than 0.01%.

The response surface model was also used to predict the result by contour plots. Contour plot is the projection of the response surface as a two dimensional plane.[44] The shapes of contour plots indicate the nature and extent of the interaction between different factors. Less prominent or negligible interactions are shown by the circular nature of the contour plots, while comparatively prominent interactions are otherwise shown by the elliptical nature of the contour plots.[45]

The response surface plots in Figure S1 illustrated the effects of pair- wise combination of the three factors, on the response. In generating these plots, one factor was kept at their center point levels. The plots in Figure S1 provide a visual indication of how any two factors interactively affected the response. Figure S1(a) illustrated the effect of varying the temperature and time of reaction with concentration of sodium hydroxide kept at constant 12 wt % while Figure. S1(b) showed effect of concentration of sodium hydroxide and temperature at constant time of 90 minutes. Figure S1(c) showed the contour

plot of concentration of sodium hydroxide and time while keeping temperature constant value of 120 ^{o} C. Overall it can be shown that all three factors temperature, concentration and time has significant effect on lignin content in (Table S6). The central points of the contour plots were used to identify the optimized conditions.

Validation of the response surface model . Validation runs were carried out with the values of the factors fixed at the identified optimized levels. (Table S7) The measured response was compared to the model equation (Eq. 3) predicted response. The measured residual lignin content measured under the optimized conditions was 8.19 %. For the same conditions, the model predicted response was 10.79 %. Therefore, the model prediction agreed with measured data within ± 2% of the measured value.

Delignification

The relevant factors in case of delignification were the concentration of sodium chlorite, temperature and time of reaction. Each factor was tested at three levels (Table S3). The center point levels were kept at the values found to be optimal via the one-at-a-time variation of factors.

The response surface model was as follows:

Lignin (%) = 22.65 + 5.20A – 0.45B - 3.47C+ 0.53AB + 0.84 AC + 1.22 BC – 2.64 A^2 – 2.75 B^2-2.53C^2.....(4)

Where A is the Temperature in ^{0}C, B is the time in minutes, C is the Concentration of sodium chlorite in wt % (Table S8).

The least residual lignin content of 6.47 % was measured in run 8 (Table S4) with the predicted value 5.44 %. The ANOVA of the response surface model (Eq. (4)) is shown in Table S9. The F-value for the model (i.e. Eq. (4)) was >12 (Table S9), suggesting that the model was significant and the probability of the F-value of the model being due to experimental noise was less than 0.02%. The temperature of the reaction and concentration of sodium chlorite had a significant effect on the response, but not the time taken for the reaction. However, the interactive effect of all the factors was insignificant (Table S9, P > 0.05). The determination coefficient (R^2) of the model (Eq. (4)) was 0.9208, therefore the model could explain >92% of the variation in the predicted response of the lignin content. In this case, the data from ANOVA (Table S9) also showed that P value was very low, smaller than 01.

The response surface plots in Figure S2 illustrate the effects of pair- wise combination of the three factors, on the response. Figure S2 (a) illustrates the effect of varying the temperature and time of reaction with concentration of sodium chlorite kept at constant 3.75wt % while Figure. S2(b) showed effect of concentration of sodium chlorite and temperature at constant time of 90 minutes. Figure S2 (c) showed the contour plot of concentration of sodium chlorite and time while keeping temperature constant value of 70 ^{o}C. Overall it can be shown that both temperature concentration had significant effect on lignin content while time seem to be having medival effect on the same as shown in Table S9.

Validation of the response surface model . Validation runs were carried out with the values of the factors fixed at the identified optimized levels. (Table S10). The measured response was compared to the model equation (Eq. 4) predicted response. The measured residual lignin content measured under the optimized conditions was 6.47 %. For the same conditions, the model predicted response was 5.44 %. Therefore, the model prediction agreed with measured data within ± 2%of the measured value.

Chemical Composition Analysis

Optimized parameters obtained through RSM was employed to prepare cellulose nanofibres. There seems to be a drastic increase in α cellulose (pure cellulose content) content from 46.5 % to 91.2 % and drop in hemicellulose (31.5% to 5.34 %) and lignin content from 21.5% to 1.32% respectively (Table 1). As seen from table, after chemical treatment most of the hemicellulose and lignin was removed from the fibres. Henceforth it is confirmed that optimized method is satisfactory.

Table1. Chemical composition analysis of rice straw components at each stage of the treatment

Material	Percentage of α cellulose	Percentage of hemicellulose	Percentage of lignin
Untreated rice straw	46.5	31.5	21.5
Alkaline cellulose fibres	72.3	17.1	10.6
Sodium chlorite treated fibres	82.64	10.99	4.97
Cellulose nanofibres	91.2	5.34	1.32

Characterization

FTIR spectroscopy

It has been extensively used in cellulose research, since it presents a relatively easy method of obtaining direct information on chemical changes that occur during chemical treatments.[46,47] Figure1 showed FT-IR spectrum of the raw rice straw fibers and chemically treated straw fibers with the aim of verifying if lignin and hemicelluloses were removed.[48] The broadened absorption band distinctive to the OH stretching was observed in all spectra in the region of 3000−3650cm^{-1}. The smaller shoulder peak at 1732cm^{-1} in the untreated rice straw F1 (Figure 1) was assigned to the characteristic of aliphatic esters in lignin and/or hemicelluloses. The peak disappears by chemical purification of the rice straw indicating near cleavage of these ester bonds.

Medchemcomm

ARTICLE

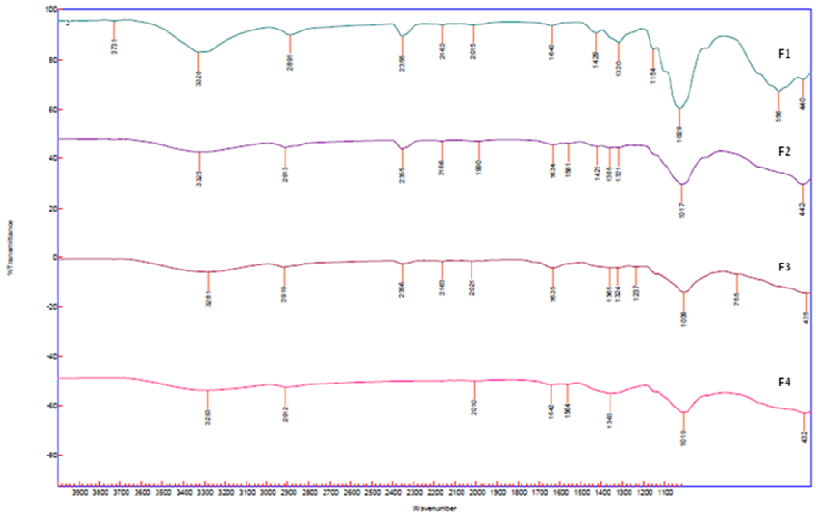

Figure 1. FTIR-ATR spectra of (F1) untreated treated rice straw (F2) alkaline cellulose fibres (F3) α cellulose (F4) Cellulose nanofibres

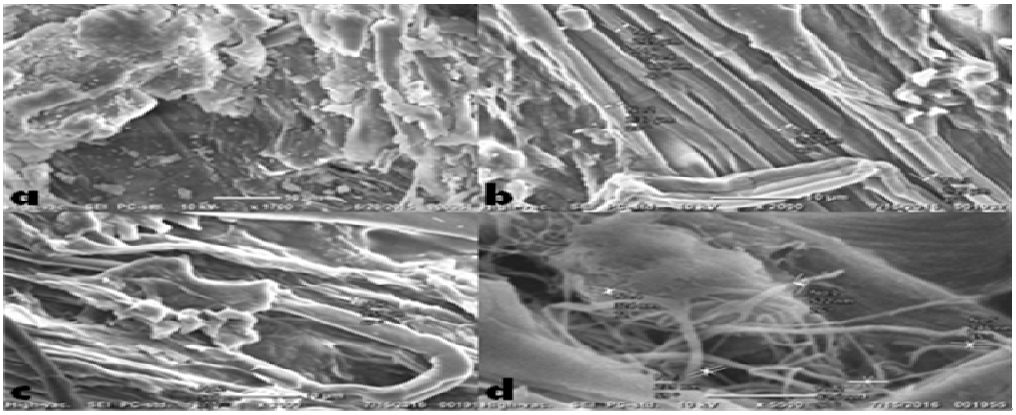

Figure 2 SEM images of (a) Rice straw (b) alkaline cellulose fibres (c) α cellulose (d) cellulose nanofibres.

Peaks at 1520 and 1459cm^{-1} were indicative of the aromatic C-C stretch of aromatic vibrations in bound lignin.[49,50] The intensity of these peaks decreased in the treated sample F2,F3,F4 (Figure 1) which evidence that the partial lignin has been removed. The absorbance peaks at 1378 and 1255cm^{-1} originate from C–H ester bands and C–O stretching vibrations due to partial acetylation of hydroxyl groups in both polysaccharides and residual lignin. The disappearance of these bands in treated fibres revealed that lignin of straw was largely removed after treatment. At 2914 cm^{-1}, a small peak was observed in samples F1, F2 and F3 which can be attributed to the aliphatic saturated C-H stretching vibration in cellulose and hemicelluloses. The absence of lignin peak in prepared CNF F4 (Figure 1) was also verified by chemical composition analysis.

Scanning Electron Microscopy (SEM):

The chemical treatments used for nanocellulose preparation from the rice straw were expected to induce morphological changes as shown by in Figure 2. Some parts of untreated rice straw were surrounded by dense lignin, hemicelluloses, and ashes, (Figure 2 a) while the surface of treated samples looked

smooth due to the removal of amorphous lignin and hemicelluloses. Chemical treatment removed the noncellulosic materials by creating structural internal tensions between the cellulose microfibers to destroy hydrogen bonds, and achieves the fibers with lower dimension.[51,52] The micrograph of alkali treated straw (Figure 2 b) showed defibrillization, fibre bundles became individualized and the microfibrils were visualized. The cementing materials (such as lignin and hemicellulose) present in the fibers got dissolved out more predominantly and the fiber length reduction took place during the bleaching process (Figure 2c). During ultrasonication and homogenization process, (Figure 2 d) a great amount of production energy released (10–100 kJ/mol), which is enough to destroy the intramolecular hydrogen bonds. Hence a combination of cellulose microfibers (1.59 µm) and nanofibers (239 nm) in the form of needle like fibres is segregated from chemically treated fibers.

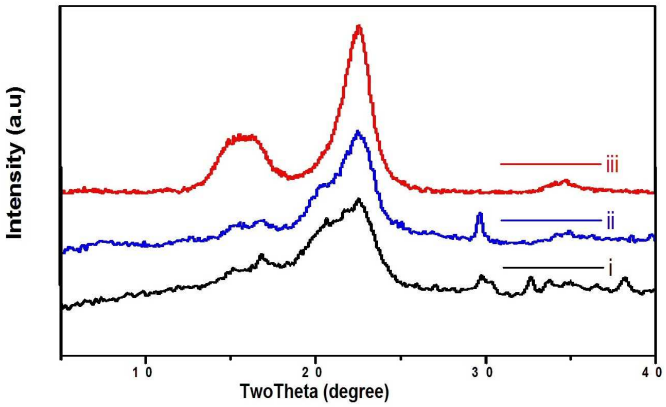

Figure 3 XRD diffraction spectra of (i) alkaline cellulose fibres (ii) α cellulose (iii) cellulose nanofibres

X-Ray diffraction

It is used to study the crystalline behaviour of fibres and to assess the relationship between structure and properties of the fiber. As cellulose is partly crystalline and partly amorphous in molecular structure, this implies that the cellulose chains will be closely held by mutual H-bonding in the crystalline (ordered) regions whereas no H-bonding occurs in the amorphous (disordered) regions of the cellulose chains. Chemical and mechanical treatments affect the crystallite size as well as the crystallinity of cellulose. So, in order to determine how crystallinity is affected by the different chemical and mechanical treatments, the crystallinity values were determined and compared between different treatments.

The X-ray diffraction patterns of the untreated and treated fibers are shown in Figure 3 shows the crystallinity of the untreated and treated fibers. It is concluded that crystallinity increases with increase in the cellulose content of the purified sample. This fact is owing to the rearrangement of natural cellulose chains after strong alkali treatment (NaOH, 12%) in stage (i). The increase in crystallinity during bleacing stage (ii) could also be attributed to the facts that the amorphous and paracrystalline cellulose regions are reorganized.

Table 2 Crystalline size and crystallinity index

S.NO.	Stages	Crystallinity index % (Eq. 1)	Crystalline size (nm) (Eq. 2)
(i)	ACF	40.84	10.00
(ii)	α cellulose	56.88	21.71
(iii)	CNF	92.08	7.53

During the sonication and homogenization process (iii), alternation between ordered and disordered cellulose fractions took place. The mechanical process has the abili to reorganize the constrained parts of the nanofibers, which were previously disordered, into crystals as a result of the increased mobility of the nanofibers in water.[53,54]

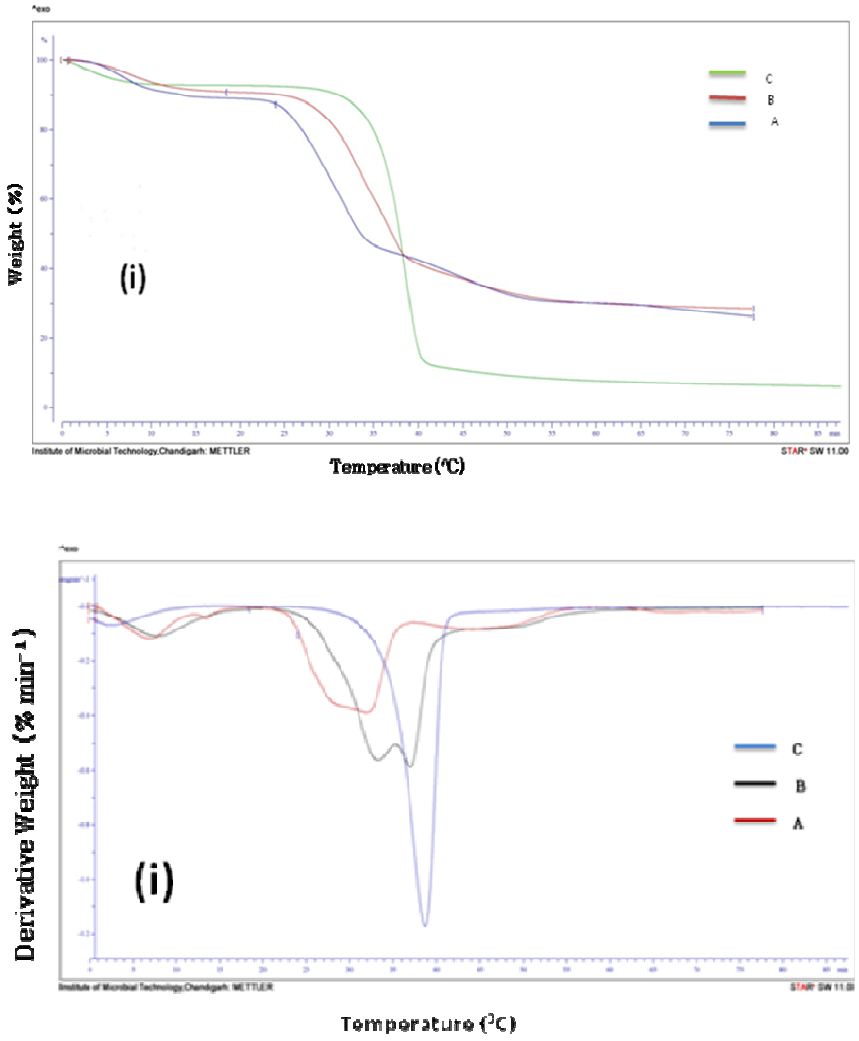

Fig 4 (i) TGA and DTG (ii) of (A) alkaline cellulose fibres, (B) α cellulose and (C) CNF prepared from rice straw**.**

The curve C of Figure 4(i) showed that the decomposition temperature of CNF was higher than the alkali treated and α cellulose respectively, as shown in Figure4 (i)(A and B). The higher temperatures of the thermal decomposition of the purified cellulose nanofibers and relatively low amount of residues are related to the partial removal of hemicelluloses, lignin, and pectin from the fibers, as well as the higher crystallinity of cellulose.[55,56] There was also a shift in peak from 260 ^{o}C to 310 ^{o}C owing to cellulose and hemicelluloses pyrolysis. These results were consistent with results obtained from crystallinity and FT-IR measurements. Figure 4(ii) showed DTG for chemically and mechanically treated fibers. Other researchers reported that in an inert atmosphere, lignin starts degrading around 200^{0} C.[57] For alkali treated rice straw fibers, the major second decomposition peak at about 321.86 ^{o}C was attributed to cellulose decomposition and the small tail peak at 343 ^{o} α cellulose may be attributed to degradation of lignin Figure 4(ii) (A,B).While in cellulosde nanofibers, DTG showed a sharp peak only at 437.58 ^{o}C indicating decomposition of crystalline cellulose Figure 4(ii) C). All these indicate that the thermal stability of treated rice straw fibers was visibly improved.

TEM images of the cellulose nanofibers were used to measure the diameters. The TEM micrographs of the nanocellulose sample, (Figure 5b) revealed that chemical and mechanical treatment resulted in defibrillation of the cellulose in the form of a network of nanofibers (as confirmed by SEM image Figure 2) from the cell wall and the separation of these nanofibers from the microsizes fiber bundles. The diameter of the fibers was found in the range of 10–50 nm. This result was in agreement with earlier studies.[59,60] A tendency of agglomeration has also been observed from TEM. It is not clear

whether this was due to high density of hydroxyl groups on the surface of cellulose chain molecules favouring the formation of hydrogen bonds or it reflected the state of the suspension.

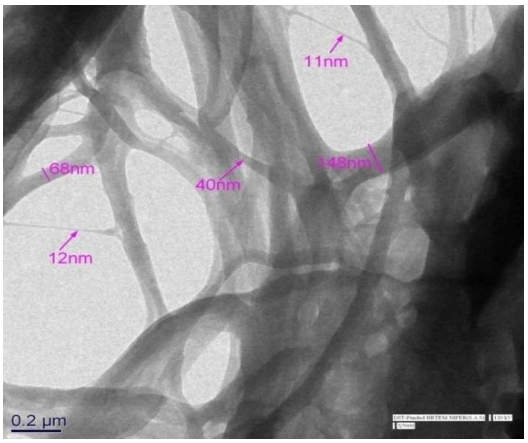

Figure 5 TEM (a) images of prepared nanocellulose showing size in the nanodimension range

Conclusions

Nanocellulose of diameter 10–50 nm were prepared from rice straw by pre-optimized process (determined through statistical method of Response Surface Methodology). During subsequent stages of the process, nanocellulose produced at the optimum chemical protocol of 12 wt% NaOH at pretreatment and 5 wt% of acidified sodium chlorite solution for delignification. Analysis showed it contained approximately 91.2% of α cellulose, 5.3% hemicellulose, and least lignin content of 1.32%. Characterization of the nanocellulose by AFM, TEM and SEM showed that fiber diameter got shorter (10-50 nm) during the sequence of treatment. The crystals of nanocellulose has a thickness of 7.53 nm with average thickness of 11 nm and the crystallinity index was 92 %. Structural analysis of cellulose nanofibres carried out by Fourier Transform Infrared (FT-IR) spectroscopy, X-ray diffraction (XRD) showed characteristic peak of α cellulose at 2 Θ=22.6 ^{0}. Further the confirmation of removal of hemicellulose and lignin was supported by the FTIR and TGA studies.

Acknowledgements

Financial support for this research from the Center of Innovative and Applied Bioprocessing, Mohali a national institute under Department of biotechnology (Govt. Of India) is greatly appreciated. The authors also acknowledge IIT, Ropar and National institute of pharmaceutical education and research, Mohali for instrumentational facilities

Notes and references

1. M. Moo-Young, *FEBS Lett.,* 1987, **220,** 387-389.
2. L. Brinchi, F. Cotana, E. Fortunati and J.M. Kenny, *Carbohydr.Polym.,* 2013, **94,** 154-169.
3. A. Dufresne, 2013, **16,** 220-227.
4. J.R McKee, S. Hietala, J. Seitsonen, J. Laine, E. Kontturi and O. Ikkala. *ACS Macro Lett.,* 2014, **3,** 266-270.
5. H.M.C. Azeredoa, M.F. Rosa, and L.H.C. Mattoso, *Ind. Crops Prod.*, 2016, **97,** 664-671.
6. Faruk, O., Sain, M., Farnood, R., Pan, Y. and Xiao, H., 2014, *J Polym Environ.,* **22,** 279.
7. D. V. Plackett, K. Letchford, J.K. Jackson and H.M. A Burt, *Nordic Pulp & Paper Research J.,* 2014, **29,** 105-118.
8. B. Xiao, X. Sun and R. Sun. *Polym. Degrad. Stab.*, 2001, **74,** 307-319.
9. X.N. Nie, J. Liu, D. She, R.C. Sun and F. Xu. *BioResources*, 2013, **8,** 3817-3832.
10. M. Jonoobi, R. Oladi, Y. Davoudpour, K. Oksman, A. Dufresne, Y. Hamzeh and R. Davoodi, 2015, *Cellulose*, **22,** 935-969.
11. C.J. Chirayil, L. Mathew and S .Thomas, *Rev. Adv. Mater. Sci.*, 2014, **37,** 20-28.
12. X. Chen, J. Yu, Z. Zhang and C. Lu. *Carbohydr. Polym.* 2011, **85,** 245-250.
13. A. Chakraborty M. Sain M. Kortschot*, Holzforschung,* 2005, **59,** 102-107.
14. A. Kaushik, M. Singh. *Carbohydr. Res.,* 2011, **346,** 76-85.
15. J. Li, X. Wei, Q. Wang, J. Chen, G. Chang, L. Kong, Y. Liu, *Carbohydr. Polym.*, 2012, **90,** 1609-1613.
16. A. Mandal and D. Chakrabarty. *Carbohydr. Polym.,* 2011, **86,** 1291-1299.
17. F. Jiang, and F. Hsieh, *Carbohydr. Polym.*, 2013, **95,** 32-40.
18. K. O. Reddy, J. Zhang and A.V. Rajulu, *Carbohydr. polym.,* 2013, **114,** 537-545.
19. G. Siqueira, S. Tapin-Lingua, Bras, J. da Silva Perez, D. Dufresne, *Cellulose*, 2010, **17,** 1147-1158.
20. F. Jiang and Y.L. Hsieh, *J. Mat. Chem. A*, 2014, **2,** 350-359.
21. A. Rattaz, S.P. Mishra, B. Chabot and C. Daneault, *Cellulose*, 2011, **18,** 585.
22. O.J. Rojas, G.A. Montero and Y. Habibi, *J .Appl. Polym. Sci,.* 2009, **113,** 927-935.
23. S. Harun, S.K. Geok, *Ind. J. Sci. Techn*. 2016, **9**.
24. M.M. Patel and R.M. Bhatt, *J. Chem. Techn. Biotech.* 1992, **53,** 253-263.
25. N.T.M. Phuong, P.H. Hoang and D.T. Hoa, *Clean Techn. Environm. Pol.*, 2017, **19,** 1313-1322.
26. P. Lu and Y. L. Hsieh, *Carbohydr. Polym*. 2012, **87,** 564-573.
27. F. Beltramino, M.B. Roncero, A.L. Torres, T. Vidal and C. Valls, *Cellulose*, 2016*,* **23,** 1777-1789.
28. L.G.J.M.A. Segal, J.J. Creely, A.E. Martin Jr and C.M. Conrad, *Text. Res. J.* 1959, **29,** 786-794.
29. H. P. Klug, L. E. Alexander, Wiley Interscience: New York, 1954.
30. J. Gu, and Y.L. Hsieh, ACS *Sustainable Chem. Eng.* 2016, 10.1021.
31. B. Nasri-Nasrabadi, T. Behzad and R. Bagheri, *J. Appl. Polym. Sci*. 2014, **131**.
32. S. Rezanezhad, N. Nooroddin and A. Ghasem. *Lignocellulose*, 2013, **2**.

33. S. Zhu, Y. Wu, Z. Yu, C. Wang, F. Yu, S. Jin, Y. Ding, R.A. Chi, J. Liao and Y. Zhang, *Biosyst. Eng.,* 2006, **93,** 279-283.
34. F. Jiang, T. Kondo and Y.L. Hsieh.*ACS Sustainable Chem. Eng*., 2016, **4,** 1697-1706.
35. M.M. Ibrahim, W.K. El-Zawawy, Y. Jüttke, A. Koschella and T. Heinze, *Cellulose*, 2013, **20,** 2403-2416.
36. D. Pasquini, E. de Morais Teixeira, A.A. da Silva Curvelo, M.N. Belgacem and A. Dufresne, *Ind. Crop Prod.*, 2010, **32,** 486-490.
37. J.H.O.D. Nascimento, R.F. Luz, F.M. Galvão, J.D.D. Melo, F.R. Oliveira, R. Ladchumananandasivam and A. Zille, *Mat. Today: proceedings*, 2015, **2,** 1-7.
38. M. Mariño, L. Lopes da Silva, N. Durán and L. Tasic, *Molecules*, 2015, **20,** 5908-5923.
39. F. Jiang and Y.L. Hsieh, *Carbohydr. Polym.* 2015, **122,** 60-68.
40. J. Gu and Y.L. Hsieh, *ACS Appl. Mater. Interfaces*, 2015, **7,** 4192-4201.
50. *Utilization, and Environmental Effects*, 2010, **33,** 114-120.
51. D. Klemm, D. Schumann, F. Kramer, N. Heßler, D. Koth and B. Sultanova, Wiley online library, 2009, **280,** 60-71.
52. F. Jiang and Y.L. Hsieh, *ACS Appl. Mater. Interfaces*, 2014, **6,** 20075-20084.
53. N. Johar, I. Ahmad and A. Dufresne, *Ind. Crops Prod.*, 2012, **37,** 93-99.
54. J.P. Reddy and J.W.Rhim, *Carbohydr. Polym.,* 2014, **110,** 480-488.
55. Y. Peng, D.J. Gardner, Y. Han, A. Kiziltas, Z. Cai and M.A. Tshabalala, *Cellulose*, 2013, **20,** 2379-2392.
41. Y. Davoudpour, S. Hossain, H.A. Khalil, M.M. Haafiz, Z.M. Ishak, A. Hassan and Z.I. Sarker, *Ind.Crops Prod.*, 2015, **74,** 381-387.
42. Z. Lu, L. Fan, H. Zheng, Q. Lu, Y. Liao and B. Huang, *Bioresou. Techno.,* 2013, **146,** 82-88.
43. M.Z. Karim, Z.Z. Chowdhury, S.B.A. Hamid and M.E. Ali, *Materials*, 2014, **7,** 6982-6999.
44. Y. Wang, H. Song, J.P. Hou, C.M. Jia and S. Yao, *Sep. Sci. Technol.*, 2013, **48,** 2217-2224.
45. G.E. Box, J.S. Hunter, *The Annals of Mathematical Statistics*, 1957, 195-241.
46. H. Sixiao, G. Jin, J. Feng, H.L. You, *ACS Sustainable Chem. Eng.* 2016, **4,** 728–737.
47. R. Sun, J. Tomkinson, F.C. Mao and X.F. Sun, *J. Appl. Polym. Sci.*, 2001, **79,** 719-732.
48. P. Garside and P. Wyeth, *Studies in Conservation*, 2003, **48,** 269-275.
49. C. Huang, L. Han, X. Liu, L. Ma, *Energy Sources, Part A: Recovery.*
56. M. Fathy, T.A. Moghny, M.A. Mousa, A.H.A. El-Bellihi and A.E. Awadallah, *Arab. J. Sci. Eng.,* 2017, **42,** 225-233.
57. M.L. Hassan, A.P. Mathew, E.A. Hassan, N.A. El-Wakil and K. Oksman, *Wood Sci. Technol.,* 2012, **46,**193-205.
58. N. Rehman, M.I.G. de Miranda, S.M. Rosa, D.M. Pimentel, S.M. Nachtigall and C.I. Bica, *J. Polym. Environ.,* 2014, **22,** 252-259.
59. R. Wagner, R.J. Moona and A.Raman, *Cellulose*, 2016, **23,** 1031-1041.
60. M.V. Zimmermann, C. Borsoi, A. Lavoratti, M. Zanini, A.J. Zattera and R.M. Santana, *J. Reinf. Plast. Comp.,* 2016, **35,** 628-643.
61. Z. Jiang, Y. Fang, Y. Ma, M. Liu, R. Liu, H. Guo, A. Lu, L. Zhang, *J. Physic. Chem. B.*, 2017, **121,** 1793-180.

AUTHOR INFORMATION

Corresponding Author
[1*]Center of Innovative and Applied Bioprocessing, Knowledge City Sector-81, Mohali, Punjab-140306.**Email:* saswata@ciab.res.in ; Tel: +: 0172-5221442

Graphical Abstract

Cellulose nanofibres From Rice Straw : Process Development For Improved Delignification And Better Crystallinity By Statistical Optimization

Amita Sharma[1], Tamal Mandal[2] and Saswata Goswami[1]*

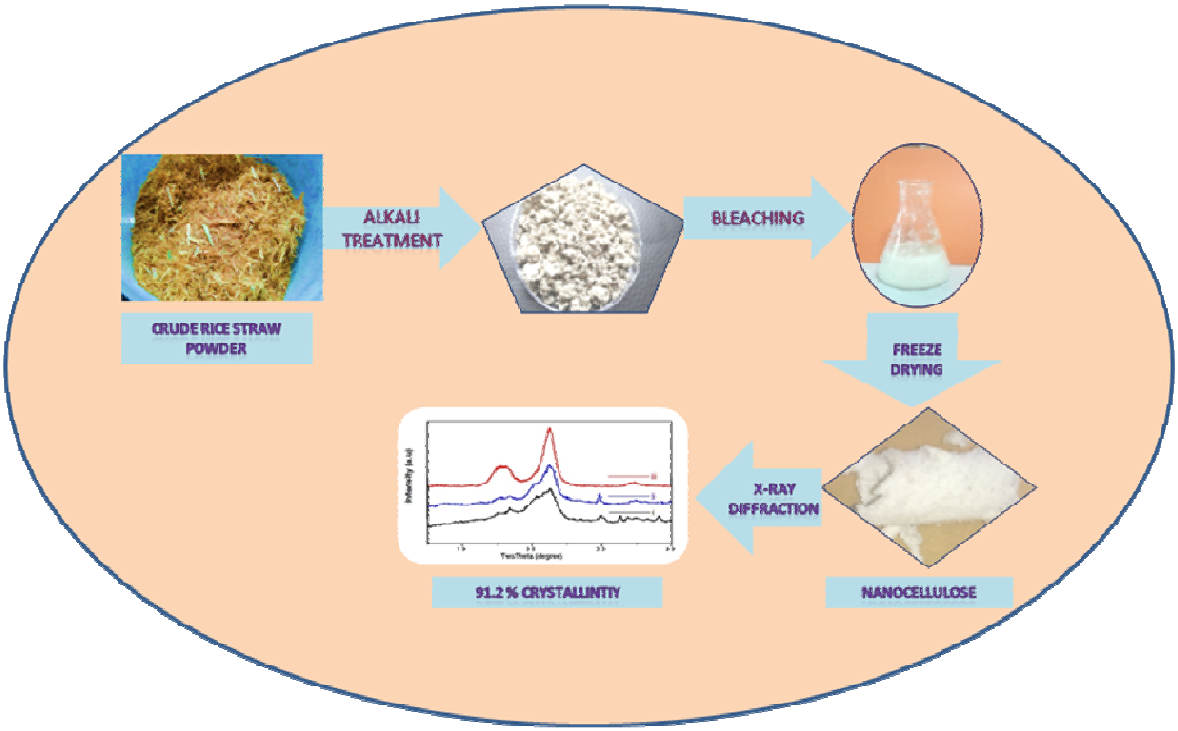

Supplementary Information

Cellulose nanofibres from rice straw : process development for improved delignification and better crystallinity index by statistical optimization

Amita Sharma[1], Tamal Mandal[2] and Saswata Goswami[1]*

[1] Center of Innovative and Applied Bioprocessing, Knowledge City Sector-81, Mohali, Punjab-140306.

[2] Department of Chemical Engineering , National institute of technology, Durgapur-Mahatma Gandhi avenue, West Bengal, Pin-713209

*Corresponding author: Email address: saswata@ciab.res.in ; Tel: +: 0172-5221442;

Add: Center of Innovative and Applied Bioprocessing, Knowledge City Sector-81, Mohali, Punjab-140306

Table of contents

Table S1 Ranges of the factors used in central composite design for pretreatment

Factors	Actual levels of coded factors		
	-1	0	1
Concentration of sodium hydroxide (wt %)	8	12	16
Time (mins)	60	90	120
Temperature (^{o}C)	90	120	160

Table S2 Experimental setup and results for the central design matrix for pretreatment

Trial No	Temperature(^{O}C)	Time(mins)	Conc. (wt%)	Lignin content (%) predicted	Lignin content (%) experimental
1	120	90	8	20.81	21.09
2	120	90	16	15.08	14.79
3	120	90	12	11.41	9.59
4	120	90	12	11.41	10.5
5	160	120	8	14.94	14.5
6	120	90	12	11.41	12.50
7	160	90	12	11.73	13.3
8	160	60	16	13.10	11.5
9	160	60	8	15.97	15.48
10	120	90	12	11.41	10.6
11	90	120	8	36.71	38.31
12	160	120	16	13.65	14.6
13	120	90	12	11.41	10.8
14	90	60	16	14.24	14.68
15	90	120	16	28.11	28.6
16	120	120	12	10.79	8.19
17	120	90	12	11.41	14.5
18	90	60	8	24.41	23.46
19	90	90	12	23.18	21.6
20	120	60	12	14.36	16.95

Table S3 Ranges of the factors used in central composite design for delignification.

Factors	Actual levels of coded factors		
	-1	0	1
Concentration of sodium chlorite (wt %)	2.5	3.75	5
Time (mins)	60	90	120
Temperature (^{o}C)	70	77.5	85

Table S4 Experimental setup and results for the central design matrix for delignification.

Trial No	Temperature(^{O}C)	Time(mins)	Conc. (wt%)	Lignin content (%) predicted	Lignin content (%) experimental
1	77.5	90	2.5	23.59	25.79
2	85	60	2.5	23.70	22.68
3	77.5	90	3.75	22.65	20.5
4	77.5	90	3.75	22.65	24.5
5	77.5	90	3.75	22.65	23.5
6	85	90	3.75	25.21	28.50
7	70	60	5	4.97	6.7
8	70	120	5	5.44	6.47
9	85	120	5	18.59	18.92
10	77.5	90	3.75	22.65	22.8
11	77.5	120	3.75	19.44	18.93
12	77.5	90	3.75	22.65	23.8
13	70	120	2.5	11.63	12.5
14	70	90	3.75	14.80	11.5
15	77.5	60	3.75	20.34	20.84
16	85	60	5	15.99	15.12
17	77.5	90	3.75	22.65	20.8
18	77.5	90	5	16.64	14.42
19	70	60	2.50	16.03	15.7
20	85	120	2.50	21.43	19.7

Table S5 Response surface model for the pretreament

	R-squared	**0.96**		**Adjusted R-squared**	**0.92**	
				95 % CI		
	Coefficient				**95 % CI**	
Factor	Estimate	df	Standard error	Low	High	VIF
Intercept	11.41	1	0.71	9.84	12.99	1
A-Temperature	5.73	1	0.65	-7.18	-4.28	1
B-Time	3.21	1	0.65	1.76	4.66	1
C-NaOH	–2.87C	1	0.65	-4.32	-1.42	1
AB	-3.33	1	0.73	-4.95	-1.71	1
AC	1.83	1	0.73	0.21	3.45	1
BC	0.39	1	0.73	-1.23	2.01	1
A^2	6.04	1	1.24	-3.28	8.80	1.82
B^2	-3.84	1	1.24	-6.6	-1.08	1.82
C^2	6.53	1	1.24	3.27	9.29	1.82

Table S6 Analysis of variance (ANOVA) for the response surface model (Eq. 3) for the pretreament.

Source	**SS**	**DF**	**MS**	**F value**	**p-value(prob>F)**
Model	1046.32	9	11.26	27.50	<0.0001
A-temperature	327.99	1	327.99	77.59	<0.001
B- Time	103.23	1	103.23	24.42	0.0006
C-concentration of sodium hydroxide	82.20	1	82.20	19.45	0.0013
AB	88.78	1	88.78	21	0.0010
AC	26.68	1	26.68	6.31	0.0308
BC	1.24	1	1.24	0.29	05999

A^2	100.29	1	100.29	23.73	0.0007
B^2	40.57	1	40.57	9.60	0.0113
C^2	117.23	1	117.23	27.73	0.0004
Residual	42.27	10	4.23		
Lack of fit	26.36	5	5.27	1.66	0.2963
Pure error	15.90	5	3.18		
Cor. Total	1088.58	19			

Sum of squares; DF—degrees of freedom; MS—mean sum of squares

Table S7 Final optimized conditions of CCD in case of pretreatment.

Factor	Name	Level	Low level	High level	Std. dev.
A	Temperature (^{O}C)	121.97	90	160	0
B	Time (mins)	90	60	120	0
C	Concentration of sodium hydroxide (wt%)	12.98	8	16	0

Table S8 Response surface model in case of delignification

	R-squared	**0.92**		**Adjusted R-squared**	**0.84**
	Coefficient			**95 % CI**	**95 % CI**
Factor	Estimate	df	Standard error	Low	High	VIF
Intercept	22.65	1	0.81	20.84	24.45	1
A-Temperature	5.20	1	0.74	3.55	6.86	1
B-Time	– 0.45	1	0.74	-2.11	1.21	1
C-NaOH	- 3.47	1	0.74	-5.39	-1.82	1
AB	0.53	1	0.83	-1.32	-2.39	1

AC	0.84	1	0.83	-1.02	3.45	1
BC	1.22	1	0.83	-0.63	3.07	1
A^2	-2.64	1	1.42	-5.80	0.52	1.82
B^2	-2.75	1	1.42	-5.91	0.41	1.82
C^2	-2.53	1	1.42	-5.69	0.63	1.82

Table S9 Analysis of variance (ANOVA) for the response surface model (Eq. 4) in case of delignification.

Source	SS	DF	MS	F value	p-value(prob>F)
Model	643.62	9	71.51	12.92	0.0002
A-temperature	270.92	1	270.92	48.95	<0.0001
B- Time	2.04	1	2.04	0.37	0.5570
C-concentration of sodium chlorite	120.69	1	120.69	21.81	0.0009
AB	2.26	1	2.26	0.41	0.5374
AC	5.59	1	5.59	1.01	0.3384
AD	11.88	1	11.88	2.15	0.1736
BC	19.13	1	19.15	3.46	0.0926
A^2	20.84	1	20.84	3.77	0.0810
B^2	17.64	1	17.64	3.19	0.1045
C^2	55.35	1			
Residual	41.81	10	5.53	3.09	0.1206
Lack of fit	15.54	5	8.36		
Pure error	55.35	5	2.71		
Cor. Total	698.96	19			

Sum of squares; DF—degrees of freedom; MS—mean sum of squares

Table S10 Final optimized conditions of CCD in case of delignification.

Factor	Name	Level	Low level	High level	Std. dev.
A	Temperature	70	70	85	0
B	Time	60	60	120	0
C	Concentration of sodium chlorite	5	2.50	5	0

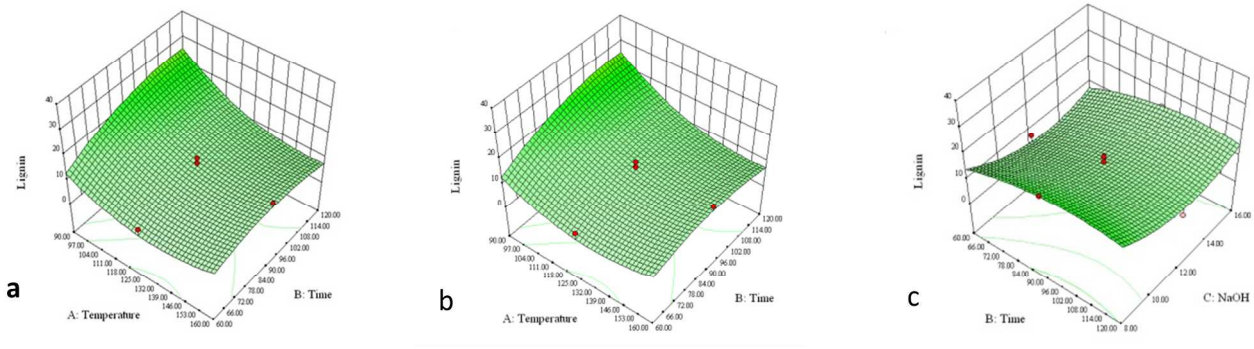

Figure S1 Response surfaces plots for the interactive effects of the following on the residual lignin content time and temperature (a) at 12 wt % concentration of sodium hydroxide; concentration of sodium hydroxide and temperature at (b) at time of 90 minutes; concentration of sodium hydroxide and time (c) at temperature of 120 ^{o}C.

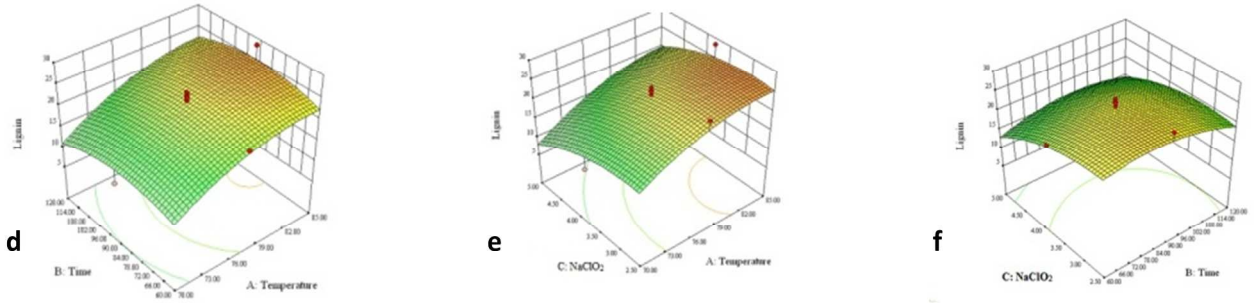

Figure S2 Response surfaces plots for the interactive effects of the following on the residual lignin content time and temperature (d) at 3.75 wt % concentration of sodium chlorite; concentration of sodium chlorite and temperature at (e) at time of 90 minutes; concentration of sodium chlorite and time (f) at temperature of 70 ^{o}C.

Letter To Referees

Dear Sir,

Sub: Submission of an original scientific research article

Please find attached herewith an original scientific research article on "**Cellulose nanofibres from rice straw: process development for improved delignification and better crystallinity index by statistical optimization**" by Amita Sharma, Tamal Mandal and Saswata Goswami for your kind consideration and peer review for publication in RSC Advances. It is further informed that all the authors have mutually agreed for its submission in this journal. This is further certified that this is an original work done by the authors and the manuscript has not been submitted earlier to this journal. As rice straw burning causes lung and respiratory diseases to the human being, soil erosion and climatic changes due to Greenhouse gas emission effect. That's why rice straw valorization is the imminent priority to the scientist. The significance of the research work lies in statistical optimization of process protocol of chemo-mechanical process for nanocellulose preparation from rice straw. The outcome of this work is that the cellulose nanofibres (CNF) has been derived with minimum lignin content of 1.32% and of better crystallinity index of 92%.

Looking forward for your kind consideration.

Thanking You,

Sincerely yours,

Saswata Goswami
Center of Innovative and Applied Bioprocessing
Knowledge City Sector-81,
Mohali, Punjab-140306.
*Corresponding author: Tel: +: 0172-5221442; saswata@ciab.res.in
Place: Mohali